Available online at www.sciencedirect.com
ScienceDirect
Computers and Mathematics with Applications 55 (2008) 2602–2622
An International Journal
computers & mathematics
with applications
www.elsevier.com/locate/camwa

Accurate and approximate analytic solutions of singularly perturbed differential equations with two-dimensional boundary layers

Zi-Cai Li[a], Heng-Shuing Tsai[a], Song Wang[b,*], John J.H. Miller[c]

[a] *Department of Applied Mathematics, Department of Computer Science and Engineering, National Sun Yat-sen University, Kaohsiung, 80424, Taiwan*
[b] *School of Mathematics and Statistics, The University of Western Australia, 35 Stirling Hwy, Crawley, WA6009, Australia*
[c] *Department of Mathematics, Trinity College, Dublin, Ireland*

Received 17 May 2007; received in revised form 4 October 2007; accepted 10 October 2007

Abstract

In this paper we construct three new test problems, called Models A, B and C, whose solutions have two-dimensional boundary layers. Approximate analytic solutions are found for these problems, which converge rapidly as the number of terms in their expansion increases. The approximations are valid for $\epsilon = 10^{-8}$ in practical computations. Surprisingly, the algorithm for Model A can be carried out even for $\epsilon \to \infty$. Model C has a simple exact solution. These three new accurate and approximate analytic solutions with two-dimensional boundary layers may be more useful for testing numerical methods than those in [Z.C. Li, H.Y. Hu, C.H. Hsu, S. Wang, Particular solutions of singularly perturbed partial differential equations with constant coefficients in rectangular domains, I. Convergence analysis, J. Comput. Appl. Math. 166 (2004) 181–208] in the sense that the series solutions from the former converge much faster than those of the latter when ϵ is small.

Keywords: Singularly perturbed equation; Boundary layer; Approximate analytic solutions; Computational models; Convergence rates

1. Introduction

There exist many reports on the study of singularly perturbed differential equations such as [2–7] to just name a few. In this paper, we follow our recent papers [8,1], and use the technique of separation of variables (cf., for example, [9]) to seek new and better test problems involving singularly perturbed differential equations. Such test problems are important for comparing the performance of various numerical methods for partial differential equations, in particular for those with singularities.

In the present paper we consider the following homogeneous equation with Dirichlet boundary conditions

$$\mathcal{L}u \equiv -\epsilon(u_{xx} + u_{yy}) + \alpha u_x + \beta u_y + cu = 0, \quad \text{in } S, \tag{1.1}$$

$$u|_\Gamma = g, \quad \text{on } \Gamma, \tag{1.2}$$

* Corresponding author.
E-mail addresses: zcli@math.nsysu.edu.tw (Z.-C. Li), swang@maths.uwa.edu.au (S. Wang), jmiller@tcd.ie (J.J.H. Miller).

0898-1221/$ - see front matter
doi:10.1016/j.camwa.2007.10.027

where S is the rectangle $S = \{(x, y), 0 < x < \pi, 0 < y < \pi\}$ and Γ is its boundary. We use the notations $u_x = \frac{\partial u}{\partial x}$ and $u_{xx} = \frac{\partial^2 u}{\partial x^2}$. The parameters ϵ, α, β and c (≥ 0) are constants, and ϵ may be arbitrarily small, $0 < \epsilon \ll 1$. We assume, without loss of generality, that

$$\alpha \geq \beta \geq 0. \tag{1.3}$$

In this case, there exist solutions with boundary layers at $x = \pi$ and $y = \pi$. Despite the restriction to constant parameters and a rectangular domain, these models are useful for testing numerical methods.

The paper is organized as follows. In the next section, we propose three test problems, called Models A, B, and C, whose solutions have two-dimensional boundary layers. In Section 3 the behaviour of their solutions is explored. In Section 4 we present an error analysis for Models A and B and error bounds are derived for their approximate solutions and approximate scaled fluxes. In Section 5 Model C is discussed. In Section 6 numerical experiments are reported, and in the last section some additional remarks are made.

Although the methods are presented in two dimensions, the idea can easily be extended to three dimensions.

2. The test problems

In this section we consider test problems that have solutions with two-dimensional boundary layers. We construct approximate solutions of these problems that have fast convergence rates. These are suitable in real computations for cases with small ϵ, for example $\epsilon = 10^{-8}$.

With the same $\mathcal{L}$ and S as in the previous section, consider the problem

$$\mathcal{L}u = 0, \quad \text{in } S, \tag{2.1}$$

$$u(x, \pi) = u(\pi, y) = 1, \tag{2.2}$$

$$u(x, 0) = g_1(x), \qquad u(0, y) = g_3(y), \tag{2.3}$$

where $u(0, 0) = 0$, $g_1(x) \in [0, 1]$ and $g_3(y) \in [0, 1]$ are smooth enough, and satisfy the following continuity conditions at the corners

$$g_1(0) = g_3(0) = 0, \qquad g_1(\pi) = g_3(\pi) = 1.$$

As in [1] we are interested in the exact solutions $\bar{u}(x, y)$ of (2.1) that satisfy the corner conditions

$$\bar{u}(0, 0) = 0, \qquad \bar{u}(\pi, 0) = \bar{u}(0, \pi) = \bar{u}(\pi, \pi) = 1. \tag{2.4}$$

In what follows we refer to such solutions as particular solutions.

2.1. Particular solutions

In order to find a suitable $\bar{u}(x, y)$ satisfying (2.4) for small values of ϵ, we seek particular solutions of (2.1) different from those in [1].

Let us first consider particular solutions depending on only one variable:

$$u = R(x), \qquad u = H(y). \tag{2.5}$$

Taking $u = R(x)$, for example, (1.1) reduces to the ordinary differential equation

$$\mathcal{L}_1 u \equiv -\epsilon u_{xx} + \alpha u_x + cu = 0, \quad \text{in } S. \tag{2.6}$$

Let $u = R(x) = \exp(\frac{\alpha}{2\epsilon}x)w(x)$. Then Eq. (2.6) becomes

$$-\epsilon w''(x) + \left(\frac{\alpha^2}{4\epsilon} + c\right) w(x) = 0 \tag{2.7}$$

and its solution is

$$w(x) = a \sinh(t_\alpha x) + b \cosh(t_\alpha x), \tag{2.8}$$

where a and b are constants, and the parameter is

$$t_\alpha = \frac{(\alpha^2 + 4\epsilon c)^{\frac{1}{2}}}{2\epsilon}. \tag{2.9}$$

Hence, the particular solutions of (2.6) are

$$R(x) = \exp\left(\frac{\alpha}{2\epsilon}x\right)\{a\sinh(t_\alpha x) + b\cosh(t_\alpha x)\}. \tag{2.10}$$

Similarly, for $u = H(y)$, we obtain the particular solutions

$$H(y) = \exp\left(\frac{\beta}{2\epsilon}y\right)\{a\sinh(t_\beta y) + b\cosh(t_\beta y)\}, \tag{2.11}$$

where

$$t_\beta = \frac{(\beta^2 + 4\epsilon c)^{\frac{1}{2}}}{2\epsilon}. \tag{2.12}$$

Next, consider separable particular solutions of the form $u = R(x)H(y)$. We have from (1.1)

$$-\epsilon\frac{R''(x)}{R} + \alpha\frac{R'(x)}{R} = \epsilon\frac{H''(y)}{H} - \beta\frac{H'(y)}{H} - c = \mu. \tag{2.13}$$

From this we see that μ must be a constant. Then we have from (2.13)

$$-\epsilon R''(x) + \alpha R'(x) = \mu R(x), \tag{2.14}$$

$$-\epsilon H''(y) + \beta H'(y) + cH(y) = -\mu H(y). \tag{2.15}$$

Under the transformation

$$R(x) = \exp\left(\frac{\alpha}{2\epsilon}x\right)v(x),$$

Eq. (2.14) leads to

$$-\epsilon v'' = \left(\mu - \frac{\alpha^2}{4\epsilon}\right)v. \tag{2.16}$$

Suppose that $\mu - \frac{\alpha^2}{4\epsilon} < 0$ (i.e., Case II in [1]). Let

$$\frac{1}{\epsilon}\left(\frac{\alpha^2}{4\epsilon} - \mu\right) = t^2, \quad t > 0. \tag{2.17}$$

Then Eq. (2.16) becomes

$$v'' - t^2 v = 0. \tag{2.18}$$

The particular solutions of (2.16) are given by

$$v = a\sinh(tx) + b\cosh(tx). \tag{2.19}$$

Now, consider (2.15), where μ in (2.17) is given by

$$\mu = \frac{\alpha^2}{4\epsilon} - \epsilon t^2.$$

Using the transformation

$$H(y) = \exp\left(\frac{\beta}{2\epsilon}y\right)w(y), \tag{2.20}$$

we obtain from (2.15)

$$-\epsilon w''(y) + \left(\frac{\alpha^2}{4\epsilon} + \frac{\beta^2}{4\epsilon} + c - \epsilon t^2\right) w(y) = 0. \tag{2.21}$$

Also, assume that $0 < t < t_0$, where t_0 in (2.33) is given by

$$t_0 = \frac{\{\alpha^2 + \beta^2 + 4\epsilon c\}^{\frac{1}{2}}}{2\epsilon}.$$

Eq. (2.21) is reduced to

$$w''(y) = (t_0^2 - t^2)w(y),$$

and its solutions are given by

$$w = \bar{a}\sinh(\sqrt{t_0^2 - t^2}y) + \bar{b}\cosh(\sqrt{t_0^2 - t^2}y), \tag{2.22}$$

where $\bar{a}$ and $\bar{b}$ are constants. Hence we have the particular solutions for (1.1)

$$u(x, y) = \exp\left(\frac{\alpha x + \beta y}{2\epsilon}\right)\{a\sinh(tx) + b\cosh(tx)\}\{\bar{a}\sinh(\sqrt{t_0^2 - t^2}y) + \bar{b}\cosh(\sqrt{t_0^2 - t^2}y)\}. \tag{2.23}$$

We choose

$$T_\alpha = \frac{(\alpha^2 + 2\epsilon c)^{\frac{1}{2}}}{2\epsilon} = t, \qquad T_\beta = \frac{(\beta^2 + 2\epsilon c)^{\frac{1}{2}}}{2\epsilon} = \sqrt{t_0^2 - t^2}, \tag{2.24}$$

and we obtain from (2.23) the particular solution

$$u(x, y) = \exp\left(\frac{\alpha x + \beta y}{2\epsilon}\right)\{a\sinh(T_\alpha x) + b\cosh(T_\alpha x)\}\{\bar{a}\sinh(T_\beta y) + \bar{b}\cosh(T_\beta y)\}. \tag{2.25}$$

By means of (2.10), (2.11) and (2.25) we obtain the following particular solution, which satisfies the corner conditions (2.4),

$$\begin{aligned}\bar{u}^*(x, y) = {} & \frac{\sinh(t_\alpha x)}{\sinh(t_\alpha \pi)}\exp\left(\frac{-\alpha(\pi - x)}{2\epsilon}\right) + \frac{\sinh(t_\beta y)}{\sinh(t_\beta \pi)} \\ & \times \exp\left(\frac{-\beta(\pi - y)}{2\epsilon}\right) - \frac{\sinh(T_\alpha x)}{\sinh(T_\alpha \pi)}\frac{\sinh(T_\beta y)}{\sinh(T_\beta \pi)}\exp\left(\frac{-\alpha(\pi - x) - \beta(\pi - y)}{2\epsilon}\right),\end{aligned} \tag{2.26}$$

where the parameters are given by

$$\begin{aligned} t_\alpha &= \frac{(\alpha^2 + 4\epsilon c)^{\frac{1}{2}}}{2\epsilon}, \qquad T_\alpha = \frac{(\alpha^2 + 2\epsilon c)^{\frac{1}{2}}}{2\epsilon}, \\ t_\beta &= \frac{(\beta^2 + 4\epsilon c)^{\frac{1}{2}}}{2\epsilon}, \qquad T_\beta = \frac{(\beta^2 + 2\epsilon c)^{\frac{1}{2}}}{2\epsilon}. \end{aligned} \tag{2.27}$$

Note that when $\epsilon \to 0$, the magnitudes of t_α and T_α are approximately equal, and similarly for t_β and T_β.

2.2. Models A, B and C

Consider the following problem with Dirichlet boundary conditions

$$\mathcal{L}u = 0, \quad \text{in } S, \tag{2.28}$$

$$u(x, \pi) = u(\pi, y) = 1, \tag{2.29}$$

$$u(x, 0) = \frac{\sinh(t_\alpha x)}{\sinh(t_\alpha \pi)}\exp\left(-\frac{\alpha(\pi - x)}{2\epsilon}\right) = \bar{u}(x, 0) = g_2(x), \tag{2.30}$$

$$u(0, y) = \frac{\sinh(t_\beta y)}{\sinh(t_\beta \pi)} \exp\left(-\frac{\beta(\pi - y)}{2\epsilon}\right) = \bar{u}(0, y) = g_4(y). \tag{2.31}$$

We define the three models as follows

Model A. Eqs. (2.28)–(2.31) with $c > 0$ and $\alpha \geq \beta > 0$.

Model B. Eqs. (2.28)–(2.31) with $c > 0$, $\alpha \geq 0$ and $\beta = 0$.

Model C. Eqs. (2.28)–(2.31) with $c = 0$, $\alpha \geq \beta > 0$.

Models A and B are convection-reaction-diffusion problems, while Model C is the convection-diffusion problems treated in [3, p. 138]. In Model A, both α and β are positive, and in Model B at least one parameter, β, is zero, so there is a parabolic layer at $y = \pi$. Equations with $c = 0$ are mainly studied in [5,4], while those with $c > 0$ are discussed in [3]. When $c = 0$ the function $\bar{u}^*(x, y)$ in (2.26) is already the solution of (2.28)–(2.31), thus there is no need for more terms in the expansion (see Section 5).

Based on [1], the solutions of (2.28)–(2.31) for both Model A and Model B are

$$u(x, y) = \bar{u}^*(x, y) + \exp\left(\frac{-\alpha(\pi - x) - \beta(\pi - y)}{2\epsilon}\right) \left\{\sum_{k=1}^{\infty} a_k^* \frac{\sinh(t_k y)}{\sinh(t_k \pi)} \sin kx + b_k^* \frac{\sinh(t_k x)}{\sinh(t_k \pi)} \sin ky\right\}, \tag{2.32}$$

where $\bar{u}^*(x, y)$ is defined in (2.26), the parameter is

$$t_k = \left\{k^2 + \frac{\alpha^2 + \beta^2 + 4\epsilon c}{4\epsilon^2}\right\}^{\frac{1}{2}}, \tag{2.33}$$

and the coefficients are

$$a_k^* = \frac{2}{\pi} \int_0^\pi (1 - \bar{u}^*(x, \pi)) \exp\left(\frac{\alpha(\pi - x)}{2\epsilon}\right) \sin kx \mathrm{d}x, \tag{2.34}$$

$$b_k^* = \frac{2}{\pi} \int_0^\pi (1 - \bar{u}^*(\pi, y)) \exp\left(\frac{\beta(\pi - y)}{2\epsilon}\right) \sin ky \mathrm{d}y. \tag{2.35}$$

In this case the coefficients (2.34) and (2.35) reduce to the explicit form, respectively,

$$a_k^* = (-1)^{k+1} \frac{kc}{\pi} \frac{\epsilon^3}{(k^2\epsilon^2 + \frac{\alpha^2 + 2c\epsilon}{4})(k^2\epsilon^2 + \frac{\alpha^2 + 4c\epsilon}{4})}, \tag{2.36}$$

$$b_k^* = (-1)^{k+1} \frac{kc}{\pi} \frac{\epsilon^3}{(k^2\epsilon^2 + \frac{\beta^2 + 2c\epsilon}{4})(k^2\epsilon^2 + \frac{\beta^2 + 4c\epsilon}{4})}. \tag{2.37}$$

We verify only (2.36), since the proof for (2.37) is similar. From (2.34) and (2.26), we have

$$a_k^* = \frac{2}{\pi} \int_0^\pi \left\{\frac{\sinh(T_\alpha x)}{\sinh(T_\alpha \pi)} - \frac{\sinh(t_\alpha x)}{\sinh(t_\alpha \pi)}\right\} \sin kx \mathrm{d}x. \tag{2.38}$$

From the integration formula in [10, p. 41]

$$\int_0^\pi \exp(px) \sin kx \mathrm{d}x = \frac{1}{(1 + \frac{p^2}{k^2})k} \{1 - (-1)^k \exp(p\pi)\}, \tag{2.39}$$

and we obtain after some manipulation

$$\int_0^\pi \frac{\sinh(T_\alpha x)}{\sinh(T_\alpha \pi)} \sin kx \mathrm{d}x = \frac{1}{\sinh(T_\alpha \pi)} \int_0^\pi \frac{\exp(T_\alpha x) - \exp(-T_\alpha x)}{2} \sin kx \mathrm{d}x = (-1)^{k+1} \frac{k}{k^2 + T_\alpha^2}. \tag{2.40}$$

Hence, using $t_\alpha^2 - T_\alpha^2 = \frac{c}{2\epsilon}$, we have from (2.38)

$$\begin{aligned} a_k^* &= (-1)^{k+1}\frac{2k}{\pi}\left\{\frac{1}{k^2+T_\alpha^2} - \frac{1}{k^2+t_\alpha^2}\right\} \\ &= (-1)^{k+1}\frac{kc}{\pi}\frac{\epsilon^3}{(k^2\epsilon^2+\frac{\alpha^2+2c\epsilon}{4})(k^2\epsilon^2+\frac{\alpha^2+4c\epsilon}{4})} \end{aligned} \tag{2.41}$$

which is (2.36).

In Model C, $c = 0$ and $a_k^* = b_k^* = 0$, for all k.

From (2.36) and (2.37) we have the following lemma.

Lemma 2.1. *Assume that $\epsilon \in (0, 1]$ is fixed. For Model A with $c > 0$, $\alpha \geq \beta > 0$, when $k \to \infty$, we have*

$$a_k^* = O\left(\frac{1}{k^3}\right), \qquad b_k^* = O\left(\frac{1}{k^3}\right). \tag{2.42}$$

Assume that k is also fixed, then for Model A, when $\epsilon \to 0$, we have

$$a_k^* = O(\epsilon^3), \qquad b_k^* = O(\epsilon^3). \tag{2.43}$$

From Lemma 2.1, we see that the coefficients in Model A are small for $\epsilon \to 0$. This is a key difference from Model I in [1].

Next, consider Model B with $c > 0$, $\alpha > 0$ and $\beta = 0$. Then we see from (2.27) and (2.33) that

$$T_\beta = \sqrt{\frac{c}{2\epsilon}}, \qquad t_\beta = \sqrt{\frac{c}{\epsilon}}, \qquad t_k = \left\{k^2 + \frac{\alpha^2+4c\epsilon}{4\epsilon^2}\right\}^{\frac{1}{2}}. \tag{2.44}$$

From (2.37) we obtain

$$b_k^* = (-1)^{k+1}\frac{c}{\pi}\frac{k\epsilon}{(k^2\epsilon+\frac{c}{2})(k^2\epsilon+c)} \tag{2.45}$$

and we have

Lemma 2.2. *Assume that $\epsilon \in (0, 1]$ is fixed. For Model B with $c > 0$, $\alpha > 0$ and $\beta = 0$, when $k \to \infty$, we have*

$$a_k^* = O\left(\frac{1}{k^3}\right), \qquad b_k^* = O\left(\frac{1}{k^3}\right). \tag{2.46}$$

Assume that k is also fixed, then for Model B with $\alpha > 0$, when $\epsilon \to 0$, we have

$$a_k^* = O(\epsilon^3), \qquad b_k^* = O(\epsilon). \tag{2.47}$$

Note that in Model B we have $b_k^* = O(\epsilon)$, in contrast to $b_k^* = O(\epsilon^3)$ in Model A.

3. Behaviour of the particular solution

We have the following proposition.

Proposition 3.1. *The particular solution $\bar{u}^*(x, y)$ defined in (2.26) satisfies the bounds*

$$0 \leq \bar{u}^*(x, y) \leq 1, \quad (x, y) \in S. \tag{3.1}$$

Proof. When $y = \pi$, we have from (2.26)

$$\bar{u}^*(x, \pi) = 1 + \left\{\frac{\sinh(t_\alpha x)}{\sinh(t_\alpha \pi)} - \frac{\sinh(T_\alpha x)}{\sinh(T_\alpha \pi)}\right\}\exp\left(\frac{-\alpha(\pi - x)}{2\epsilon}\right). \tag{3.2}$$

Introduce the function

$$f(x) = \frac{\sinh(t_\alpha x)}{\sinh(t_\alpha \pi)} - \frac{\sinh(T_\alpha x)}{\sinh(T_\alpha \pi)}. \tag{3.3}$$

We assume for the moment that

$$f(x) \le 0, \quad 0 \le x \le \pi. \tag{3.4}$$

From (3.2) and (3.4) we have

$$\bar{u}^*(x, \pi) \le 1, \quad 0 \le x \le \pi. \tag{3.5}$$

Moreover,

$$\bar{u}^*(x, \pi) \ge 1 - \frac{\sinh(T_\alpha x)}{\sinh(T_\alpha \pi)} \exp\left(\frac{-\alpha(\pi - x)}{2\epsilon}\right) \ge 0. \tag{3.6}$$

Combining (3.5) and (3.6) gives

$$0 \le \bar{u}^*(x, \pi) \le 1. \tag{3.7}$$

Similarly, we have

$$0 \le \bar{u}^*(\pi, y) \le 1, \qquad 0 \le \bar{u}^*(x, 0) \le 1, \qquad 0 \le \bar{u}^*(0, y) \le 1. \tag{3.8}$$

Hence

$$0 \le \bar{u}^*(x, y)|_\Gamma \le 1. \tag{3.9}$$

Since the maximal and minimal values of $\bar{u}^*(x, y)$ occur only along Γ for singularly perturbed partial differential equations with homogeneous right-hand sides, see [5,1], the desired result (3.1) follows. It remains to prove (3.4), which we do by contradiction. From (3.3), $f(0) = f(\pi) = 0$. Suppose that there exists a point $\xi \in (0, \pi)$ such that

$$f(\xi) > 0. \tag{3.10}$$

From the Lagrange mean value theorem, there must exist two points η_1 and η_2 with $0 < \eta_1 < \xi < \eta_2 < \pi$ such that

$$f'(\eta_1) = \frac{f(\xi) - f(0)}{\xi} > 0, \qquad f'(\eta_2) = \frac{f(\pi) - f(\xi)}{\pi - \xi} < 0. \tag{3.11}$$

From (3.3)

$$f'(\eta_1) = \frac{t_\alpha \cosh(t_\alpha \eta_1)}{\sinh(t_\alpha \pi)} - \frac{T_\alpha \cosh(T_\alpha \eta_1)}{\sinh(T_\alpha \pi)} > 0, \tag{3.12}$$

$$f'(\eta_2) = \frac{t_\alpha \cosh(t_\alpha \eta_2)}{\sinh(t_\alpha \pi)} - \frac{T_\alpha \cosh(T_\alpha \eta_2)}{\sinh(T_\alpha \pi)} < 0.$$

Then

$$\frac{t_\alpha \sinh(T_\alpha \pi)}{T_\alpha \sinh(t_\alpha \pi)} > \frac{\cosh(T_\alpha \eta_1)}{\cosh(t_\alpha \eta_1)}, \qquad \frac{t_\alpha \sinh(T_\alpha \pi)}{T_\alpha \sinh(t_\alpha \pi)} < \frac{\cosh(T_\alpha \eta_2)}{\cosh(t_\alpha \eta_2)}. \tag{3.13}$$

This leads to

$$\frac{\cosh(T_\alpha \eta_1)}{\cosh(t_\alpha \eta_1)} < \frac{\cosh(T_\alpha \eta_2)}{\cosh(t_\alpha \eta_2)}, \quad \eta_1 < \eta_2. \tag{3.14}$$

Introduce the function

$$g(\eta) = \frac{\cosh(T_\alpha \eta)}{\cosh(t_\alpha \eta)}. \tag{3.15}$$

By the mean value theorem again, from (3.14) and (3.15) we have

$$g(\eta_2) - g(\eta_1) = g'(\bar{\eta})(\eta_2 - \eta_1), \tag{3.16}$$

where $\eta_1 < \bar{\eta} < \eta_2$, and so $g'(\bar{\eta}) > 0$. On the other hand, since $0 < T_\alpha < t_\alpha$, we have

$$\begin{aligned} g'(\bar{\eta}) &= \frac{T_\alpha \sinh(T_\alpha\bar{\eta})\cosh(t_\alpha\bar{\eta}) - t_\alpha \sinh(t_\alpha\bar{\eta})\cosh(T_\alpha\bar{\eta})}{(\cosh(t_\alpha\bar{\eta}))^2} \\ &\le t_\alpha \frac{\sinh(T_\alpha\bar{\eta})\cosh(t_\alpha\bar{\eta}) - \sinh(t_\alpha\bar{\eta})\cosh(T_\alpha\bar{\eta})}{(\cosh(t_\alpha\bar{\eta}))^2} \\ &= t_\alpha \frac{\sinh((T_\alpha - t_\alpha)\bar{\eta})}{(\cosh(t_\alpha\bar{\eta}))^2} < 0 \end{aligned} \tag{3.17}$$

which contradicts the above. Thus Eq. (3.4) holds. This completes the proof of Proposition 3.1. ■

The bounds on $\bar{u}^*(x, y)$ in the above proposition are important, because they guarantee that in this case there is no serious numerical instability or additional computational work. This is in contrast to the case for Model I in [1] for which the function $\bar{u}(x, y) = O(\exp(\frac{\alpha}{2\epsilon}))$.

We now introduce $w = u - \bar{u}^*$. It is easy to see that w is the solution of the problem

$$\mathcal{L}w = 0, \quad \text{in } S, \tag{3.18}$$

$$w(x, 0) = w(0, y) = 0, \tag{3.19}$$

$$\begin{aligned} w(x, \pi) &= 1 - \bar{u}^*(x, \pi) = f_2(x) \\ &= \left\{ \frac{\sinh(T_\alpha x)}{\sinh(T_\alpha \pi)} - \frac{\sinh(t_\alpha x)}{\sinh(t_\alpha \pi)} \right\} \exp\left(-\frac{\alpha(\pi - x)}{2\epsilon} \right), \end{aligned} \tag{3.20}$$

$$\begin{aligned} w(\pi, y) &= 1 - \bar{u}^*(\pi, y) = f_4(y) \\ &= \left\{ \frac{\sinh(T_\beta y)}{\sinh(T_\beta \pi)} - \frac{\sinh(t_\beta y)}{\sinh(t_\beta \pi)} \right\} \exp\left(-\frac{\beta(\pi - y)}{2\epsilon} \right). \end{aligned} \tag{3.21}$$

The following propositions give bounds on w for Models A and B.

Proposition 3.2. *For Model A with $\alpha \ge \beta > 0$ and $c > 0$, when $\epsilon \to 0$, there exists the approximate bound*

$$|w(x, y)| \le C_A \approx \frac{c\epsilon}{2\mathrm{e}} \max\left\{ \frac{1}{\alpha^2}, \frac{1}{\beta^2} \right\}, \quad (x, y) \in S. \tag{3.22}$$

Proof. Since the maximal and minimal values of w occur on Γ, we seek the extremes of the functions $f_2(x)$ and $f_4(y)$. Let $x = \bar{x}$ be a stationary point of $f_2(x)$, then

$$0 = f_2'(\bar{x}) = \left\{ \frac{\frac{\alpha}{2\epsilon}\sinh(T_\alpha\bar{x}) + T_\alpha\cosh(T_\alpha\bar{x})}{\sinh(T_\alpha\pi)} - \frac{\frac{\alpha}{2\epsilon}\sinh(t_\alpha\bar{x}) + t_\alpha\cosh(t_\alpha\bar{x})}{\sinh(t_\alpha\pi)} \right\} \exp\left(-\frac{\alpha(\pi - \bar{x})}{2\epsilon} \right). \tag{3.23}$$

Moreover, since for $\epsilon \to 0$, $t_\alpha \to \infty$ and

$$\sinh(t_\alpha\bar{x}) \approx \frac{1}{2}\exp(t_\alpha\bar{x}), \qquad \cosh(t_\alpha\bar{x}) \approx \frac{1}{2}\exp(t_\alpha\bar{x}), \tag{3.24}$$

we obtain from (3.23)

$$\left(\frac{\alpha}{2\epsilon} + T_\alpha \right) \exp(T_\alpha(\bar{x} - \pi)) \approx \left(\frac{\alpha}{2\epsilon} + t_\alpha \right) \exp(t_\alpha(\bar{x} - \pi)). \tag{3.25}$$

When $\epsilon \to 0$, we also have the approximation for (2.24)

$$T_\alpha = \frac{\{\alpha^2 + 2c\epsilon\}^{\frac{1}{2}}}{2\epsilon} = \frac{\alpha}{2\epsilon}\left\{ 1 + \frac{2c\epsilon}{\alpha^2} \right\}^{\frac{1}{2}} \approx \frac{\alpha}{2\epsilon}\left(1 + \frac{c\epsilon}{\alpha^2} \right), \tag{3.26}$$

and

$$t_\alpha = \frac{\{\alpha^2 + 4c\epsilon\}^{\frac{1}{2}}}{2\epsilon} \approx \frac{\alpha}{2\epsilon}\left(1 + \frac{2c\epsilon}{\alpha^2} \right). \tag{3.27}$$

Eq. (3.25) reduces approximately to

$$\frac{1+\frac{c\epsilon}{2\alpha^2}}{1+\frac{c\epsilon}{\alpha^2}} \approx \exp\left(\frac{c}{2\alpha}(\bar{x}-\pi)\right). \tag{3.28}$$

Let $\bar{x} = \pi - \nu\epsilon$, where ν is a constant independent of ϵ. Then for $\epsilon \to 0$, we have from (3.28)

$$\nu \approx \frac{1}{\alpha}. \tag{3.29}$$

Hence, when $\bar{x} = \pi - \frac{\epsilon}{\alpha}$, we obtain the approximate maximal values

$$\begin{aligned} |w(x,\pi)| &\le |f_2(\bar{x})| = |w(\bar{x},\pi)| \\ &= \left\{\frac{\sinh(T_\alpha \bar{x})}{\sinh(T_\alpha \pi)} - \frac{\sinh(t_\alpha \bar{x})}{\sinh(t_\alpha \pi)}\right\} \exp\left(-\frac{\alpha(\pi-\bar{x})}{2\epsilon}\right) \\ &\approx \mathrm{e}^{-\frac{1}{2}}\left\{\exp\left(-\frac{1}{2}\left(1+\frac{c\epsilon}{\alpha^2}\right)\right) - \exp\left(-\frac{1}{2}\left(1+\frac{2c\epsilon}{\alpha^2}\right)\right)\right\} \\ &\approx \frac{1}{2\mathrm{e}}\frac{c\epsilon}{\alpha^2}, \quad \alpha > 0. \end{aligned} \tag{3.30}$$

Similarly,

$$|w(\pi,y)| \le C_A \approx \frac{1}{2\mathrm{e}}\frac{c\epsilon}{\beta^2}, \quad \beta > 0. \tag{3.31}$$

The desired result (3.22) follows. This completes the proof of Proposition 3.2. ■

Proposition 3.3. *For Model B with $\alpha > 0$, $\beta = 0$ and $c > 0$, when $\epsilon \to 0$, there exists for all $(x, y) \in S$ the approximate bound*

$$|w(x,y)| \le C_B \approx 0.1268. \tag{3.32}$$

Proof. When $\beta = 0$, $t_\beta = \sqrt{\frac{c}{\epsilon}}$ and $T_\beta = \sqrt{\frac{c}{2\epsilon}}$. We have from (3.21) for $x = \pi$,

$$f_4(y) = w(\pi,y) = \frac{\sinh(\sqrt{\frac{c}{2\epsilon}}y)}{\sinh(\sqrt{\frac{c}{2\epsilon}}\pi)} - \frac{\sinh(\sqrt{\frac{c}{\epsilon}}y)}{\sinh(\sqrt{\frac{c}{\epsilon}}\pi)}. \tag{3.33}$$

The stationary point $\bar{y}$ is located by

$$0 = f_4'(\bar{y}) = \sqrt{\frac{c}{2\epsilon}}\frac{\cosh(\sqrt{\frac{c}{2\epsilon}}\bar{y})}{\sinh(\sqrt{\frac{c}{2\epsilon}}\pi)} - \sqrt{\frac{c}{\epsilon}}\frac{\cosh(\sqrt{\frac{c}{\epsilon}}\bar{y})}{\sinh(\sqrt{\frac{c}{\epsilon}}\pi)}. \tag{3.34}$$

This gives for $\epsilon \to 0$,

$$\sqrt{\frac{c}{2\epsilon}}\exp\left(\sqrt{\frac{c}{2\epsilon}}(\bar{y}-\pi)\right) \approx \sqrt{\frac{c}{\epsilon}}\exp\left(\sqrt{\frac{c}{\epsilon}}(\bar{y}-\pi)\right). \tag{3.35}$$

Let $\bar{y} = \pi - \nu\sqrt{\frac{\epsilon}{c}}$. We have from (3.35)

$$\sqrt{\frac{c}{2\epsilon}}\exp\left(-\frac{\nu}{\sqrt{2}}\right) \approx \sqrt{\frac{c}{\epsilon}}\exp(-\nu). \tag{3.36}$$

This gives

$$\nu \approx \frac{\ln\sqrt{2}}{1-\frac{1}{\sqrt{2}}} = \frac{\ln 2}{2-\sqrt{2}} = 1.1833. \tag{3.37}$$

For $\bar{y} = \pi - \nu\sqrt{\frac{\epsilon}{c}}$, we obtain the approximation

$$f_4(\bar{y}) = w(\pi, \bar{y}) = \frac{\sinh(\sqrt{\frac{c}{2\epsilon}}\bar{y})}{\sinh(\sqrt{\frac{c}{2\epsilon}}\pi)} - \frac{\sinh(\sqrt{\frac{c}{\epsilon}}\bar{y})}{\sinh(\sqrt{\frac{c}{\epsilon}}\pi)}$$
$$\approx \exp\left(-\frac{\nu}{\sqrt{2}}\right) - \exp(-\nu) = 0.1268. \tag{3.38}$$

Also, since the maximal values occur on the boundary Γ, we have for $\epsilon \to 0$

$$|w(x, y)| \le C_B \approx \max\left\{0.1268, \frac{1}{2\mathrm{e}}\frac{c\epsilon}{\alpha^2}\right\} = 0.1268. \tag{3.39}$$

This completes the proof of Proposition 3.3. ■

Propositions 3.2 and 3.3 suggest different rates of convergence, as $\epsilon \to 0$, for Models A and B, details of which are provided in the next section. Note that, as $\epsilon \to 0$, the width $O(\sqrt{\epsilon})$ of the parabolic boundary layers is much wider than the width $O(\epsilon)$ of the regular boundary layers in singularly perturbed partial differential equations.

4. Convergence analysis for Models A and B

In practical computations, in order to obtain approximate solutions we must take a finite number of terms in (2.32)

$$u_N(x, y) = \bar{u}^*(x, y) + \exp\left(\frac{-\alpha(\pi - x) - \beta(\pi - y)}{2\epsilon}\right) \times \left\{\sum_{k=1}^{N} a_k^* \frac{\sinh(t_k y)}{\sinh(t_k \pi)} \sin kx + b_k^* \frac{\sinh(t_k x)}{\sinh(t_k \pi)} \sin ky\right\}. \tag{4.1}$$

Therefore we need a convergence analysis for Models A and B in order to derive a bound on $|u - u_N|$ for the solution error and bounds on $|(u_x - (u_N)_x)|$ and $|(u_y - (u_N)_y)|$ for the flux errors.

4.1. Error bound for the solution of Models A and B

We have the following theorem, which provides a bound on the solution error $|u - u_N|$.

Theorem 4.1. *For Models A and B we have*

$$\max_S |u - u_N| \le \frac{c\epsilon}{2\pi}\left\{\frac{1}{\epsilon^2 N^2 + \frac{\alpha^2 + 2c\epsilon}{4}} + \frac{1}{\epsilon^2 N^2 + \frac{\beta^2 + 2c\epsilon}{4}}\right\} \exp\left(\frac{-\alpha(\pi - x) - \beta(\pi - y)}{2\epsilon}\right). \tag{4.2}$$

Proof. We have from (4.1) and (2.32)

$$|u - u_N| = \exp\left(\frac{-\alpha(\pi - x) - \beta(\pi - y)}{2\epsilon}\right) \sum_{k=N+1}^{\infty} \left| a_k^* \frac{\sinh(t_k y)}{\sinh(t_k \pi)} \sin kx + b_k^* \frac{\sinh(t_k x)}{\sinh(t_k \pi)} \sin ky \right|$$
$$\le \exp\left(\frac{-\alpha(\pi - x) - \beta(\pi - y)}{2\epsilon}\right) \sum_{k=N+1}^{\infty} (|a_k^*| + |b_k^*|). \tag{4.3}$$

From (2.36) and (2.37) we obtain

$$|a_k^*| \le \frac{kc}{\pi} \frac{\epsilon^3}{(k^2\epsilon^2 + \frac{\alpha^2 + 2c\epsilon}{4})^2}, \qquad |b_k^*| \le \frac{kc}{\pi} \frac{\epsilon^3}{(k^2\epsilon^2 + \frac{\beta^2 + 2c\epsilon}{4})^2}. \tag{4.4}$$

Then we have

$$\sum_{k=N+1}^{\infty} |a_k^*| \le \frac{c\epsilon^2}{\pi} \sum_{k=N+1}^{\infty} \frac{k\epsilon}{(k^2\epsilon^2 + \frac{\alpha^2+2c\epsilon}{4})^2} \le \frac{c\epsilon^2}{\pi} \int_N^{\infty} \frac{\epsilon t \,\mathrm{d}t}{(t^2\epsilon^2 + \frac{\alpha^2+2c\epsilon}{4})^2}. \tag{4.5}$$

From calculus we obtain

$$\int_N^{\infty} \frac{\epsilon t}{\left(t^2\epsilon^2 + \frac{\alpha^2+2c\epsilon}{4}\right)^2} \mathrm{d}t = \frac{1}{2\epsilon} \frac{1}{N^2\epsilon^2 + \frac{\alpha^2+2c\epsilon}{4}}. \tag{4.6}$$

Hence

$$\sum_{k=N+1}^{\infty} |a_k^*| \le \frac{c}{2\pi} \frac{\epsilon}{N^2\epsilon^2 + \frac{\alpha^2+2c\epsilon}{4}}. \tag{4.7}$$

Similarly

$$\sum_{k=N+1}^{\infty} |b_k^*| \le \frac{c}{2\pi} \frac{\epsilon}{N^2\epsilon^2 + \frac{\beta^2+2c\epsilon}{4}}. \tag{4.8}$$

The required result (4.2) is obtained from (4.3), (4.7) and (4.8). ■

For $\alpha \ge \beta > 0$, when $N = 0$, we have from Theorem 4.1

$$|(u - \bar{u}^*)(x, y)| \equiv |w(x, y)| \le \frac{2c\epsilon}{\pi} \left\{ \frac{1}{\alpha^2} + \frac{1}{\beta^2} \right\}. \tag{4.9}$$

Comparing the constants in Proposition 3.2 and Theorem 4.1, the same parameters $O(\frac{c\epsilon}{\alpha^2})$ and $O(\frac{c\epsilon}{\beta^2})$ are found. However, the factor $\frac{2}{\pi} = 0.6366$ in Theorem 4.1 is larger than the factor $\frac{1}{2e} = 0.1839$ in Proposition 3.2. Moreover in Model B with $\beta = 0$, $\alpha \ge 0$, $c > 0$ and $N = 0$, we have from Theorem 4.1

$$|u - \bar{u}^*| \equiv |w(x, y)| \le \frac{1}{\pi} = 0.3183, \tag{4.10}$$

which is also larger than the 0.1268 obtained from Proposition 3.3.

For approximations to the solution u we choose N to fulfill the criterion

$$\max_S |u - u_N| \le \delta = \frac{1}{2} 10^{-4}. \tag{4.11}$$

This ensures that at least four significant digits in the mantissa must be correct for the u_N close to the boundary $x = \pi$ and $y = \pi$, since $\max_S |u(x, y)| = 1$ and $u_N = 1$ at $x = \pi \cup y = \pi$.

We have the following corollaries from Theorem 4.1.

Corollary 4.1. *For Model B with $\beta = 0$, (4.11) is satisfied if we choose*

$$N = \sqrt{\frac{c}{\pi\epsilon\delta}}. \tag{4.12}$$

Often in practical computations, we choose N as large as $N = O(10^6)$. Then, in (4.12), $\epsilon = 10^{-8}$ can be allowed, which is satisfactory for many practical applications.

Corollary 4.2. *For Model A with $\alpha \ge \beta > 0$, when $\epsilon \ge \frac{\delta}{q}$ with the constant $q = \frac{4c}{\pi\beta^2}$, (4.11) is satisfied if we choose*

$$N = \sqrt{\frac{c}{\pi\epsilon\delta}} = O(10^4). \tag{4.13}$$

Also, when $\epsilon \le \frac{\delta}{q}$, it suffices to choose

$$N = O(1) \quad or \quad N = 0. \tag{4.14}$$

Proof. We show only (4.14). From (4.2) and $\epsilon \le \frac{\delta}{q}$, we have

$$\max_S |u - u_N| \le \frac{c\epsilon}{\pi\left(\epsilon^2 N^2 + \frac{\beta^2+2c\epsilon}{4}\right)} \le \frac{4c\epsilon}{\pi\beta^2} = q\epsilon \le \delta. \tag{4.15}$$

Corollary 4.2 implies that Model A may serve as a better test problem than Model B, because the N can be chosen to be moderately small, and particularly, we may choose $N = 0$ (i.e., $u_0(x, y) = \bar{u}^*(x, y)$) when $\epsilon \to 0$. This surprising result also agrees with Proposition 3.2. ■

4.2. Error bounds for the scaled fluxes in Models A and B

We now establish bounds for the appropriately scaled errors in the fluxes $|(u_x - (u_N)_x)|$ and $|(u_y - (u_N)_y)|$. From (4.1) we have the approximate derivatives

$$(u_N)_x = \bar{u}^*_x(x, y) + \exp\left(\frac{-\alpha(\pi - x) - \beta(\pi - y)}{2\epsilon}\right)\left\{\frac{\alpha}{2\epsilon}\sum_{k=1}^{N}\left(a^*_k \frac{\sinh(t_k y)}{\sinh(t_k\pi)}\sin kx + b^*_k \frac{\sinh(t_k x)}{\sinh(t_k\pi)}\sin ky\right)\right.$$
$$\left. + \sum_{k=1}^{N}\left(a^*_k k \frac{\sinh(t_k y)}{\sinh(t_k\pi)}\cos kx + b^*_k t_k \frac{\cosh(t_k x)}{\sinh(t_k\pi)}\sin ky\right)\right\}, \tag{4.16}$$

and

$$(u_N)_y = \bar{u}^*_y(x, y) + \exp\left(\frac{-\alpha(\pi - x) - \beta(\pi - y)}{2\epsilon}\right)\left\{\frac{\beta}{2\epsilon}\sum_{k=1}^{N}\left(a^*_k \frac{\sinh(t_k y)}{\sinh(t_k\pi)}\sin kx + b^*_k \frac{\sinh(t_k x)}{\sinh(t_k\pi)}\sin ky\right)\right.$$
$$\left. + \sum_{k=1}^{N}\left(a^*_k t_k \frac{\cosh(t_k y)}{\sinh(t_k\pi)}\sin kx + b^*_k k \frac{\sinh(t_k x)}{\sinh(t_k\pi)}\cos ky\right)\right\}. \tag{4.17}$$

We have the following theorem for Models A and B.

Theorem 4.2. *Let $\epsilon \in (0, 1]$. For Models A and B, we have the error bound*

$$\max_S |\epsilon(u_x - (u_N)_x)| \le \frac{3}{1 - \exp(-(\frac{\beta}{2} + \sqrt{c})\pi)} \times \left\{\frac{c}{\pi N} + \frac{(\frac{\alpha}{\sqrt{2}} + \sqrt{c})c}{\pi}\left\{\frac{\epsilon}{\epsilon^2 N^2 + \frac{\beta^2+2c\epsilon}{4}}\right\}\right\}\exp\left(\frac{-\alpha(\pi - x) - \beta(\pi - y)}{2\epsilon}\right). \tag{4.18}$$

Proof. We have from (4.16) and (2.32)

$$|u_x - (u_N)_x| \le \frac{\alpha}{2\epsilon}|u - u_N| + \sum_{k=N+1}^{\infty}\left(|a^*_k|k + |b^*_k|t_k \frac{\cosh(t_k x)}{\sinh(t_k\pi)}\right)\exp\left(\frac{-\alpha(\pi - x) - \beta(\pi - y)}{2\epsilon}\right). \tag{4.19}$$

The bound on the first term on the right-hand side of (4.19) is obtained from Theorem 4.1

$$\frac{\alpha}{2\epsilon}|u - u_N| \le \frac{\alpha c}{2\pi}\left\{\frac{1}{\epsilon^2 N^2 + \frac{\beta^2+2c\epsilon}{4}}\right\}\exp\left(\frac{-\alpha(\pi - x) - \beta(\pi - y)}{2\epsilon}\right). \tag{4.20}$$

Next, we have from (2.36)

$$\sum_{k=N+1}^{\infty} |a_k^*| k \le \frac{c}{\pi} \sum_{k=N+1}^{\infty} \frac{k^2\epsilon^3}{(k^2\epsilon^2 + \frac{\alpha^2+2c\epsilon}{4})^2} \le \frac{c}{\pi\epsilon} \sum_{k=N+1}^{\infty} \frac{1}{k^2} \le \frac{c}{\pi\epsilon} \int_N^{\infty} \frac{\mathrm{d}t}{t^2} = \frac{c}{\pi\epsilon N}. \tag{4.21}$$

Also, for $\epsilon \le 1$ and $\alpha \ge \beta$, we have from $\sqrt{a^2+b^2} \le |a| + |b|$,

$$t_k = \left\{ k^2 + \frac{\alpha^2+\beta^2+4\epsilon c}{4\epsilon^2} \right\}^{\frac{1}{2}} \le k + \frac{1}{\epsilon}\left(\frac{\alpha}{\sqrt{2}} + \sqrt{c\epsilon}\right) \le k + \frac{1}{\epsilon}\left(\frac{\alpha}{\sqrt{2}} + \sqrt{c}\right). \tag{4.22}$$

Then, we obtain the bound

$$\sum_{k=N+1}^{\infty} |b_k^*| t_k \le \sum_{k=N+1}^{\infty} k|b_k^*| + \frac{1}{\epsilon}\left(\frac{\alpha}{\sqrt{2}} + \sqrt{c}\right) \sum_{k=N+1}^{\infty} |b_k^*|. \tag{4.23}$$

From similar arguments to those used for (4.21) and from Theorem 4.1, we see that

$$\sum_{k=N+1}^{\infty} |b_k^*| t_k \le \left\{ \frac{c}{\pi\epsilon N} + \frac{(\frac{\alpha}{\sqrt{2}} + \sqrt{c})c}{\pi} \frac{1}{\epsilon N^2 + \frac{\beta^2+2\epsilon c}{4}} \right\}. \tag{4.24}$$

We now consider the function

$$p(x) = \frac{\cosh(t_k x)}{\sinh(t_k \pi)}. \tag{4.25}$$

Since $p'(x) \ge 0$, the maximal value of $p(x)$ occurs at $x = \pi$, and so

$$p(x) \le \frac{\cosh(t_k\pi)}{\sinh(t_k\pi)} = \frac{1+\exp(-2t_k\pi)}{1-\exp(-2t_k\pi)} \le \frac{2}{1-\exp(-2t_k\pi)}. \tag{4.26}$$

For $\epsilon \in (0, 1]$, we have from (4.22) and $\sqrt{a^2+b^2} \ge \frac{1}{2}(|a| + |b|)$

$$t_k \ge \sqrt{\frac{\beta^2}{4\epsilon^2} + \frac{c}{\epsilon}} \ge \sqrt{\frac{\beta^2}{4} + c} \ge \frac{1}{2}\left(\frac{\beta}{2} + \sqrt{c}\right). \tag{4.27}$$

Hence we have

$$\frac{\cosh(t_k x)}{\sinh(t_k\pi)} \le \frac{2}{1-\exp\left(-\left(\frac{\beta}{2} + \sqrt{c}\right)\pi\right)}. \tag{4.28}$$

Combining (4.24) and (4.28) gives

$$\sum_{k=N+1}^{\infty} |b_k^*| t_k \frac{\cosh(t_k x)}{\sinh(t_k\pi)} \le \frac{2}{1-\exp(-(\frac{\beta}{2} + \sqrt{c})\pi)} \left\{ \frac{c}{\pi\epsilon N} + \frac{(\frac{\alpha}{\sqrt{2}} + \sqrt{c})c}{\pi} \frac{1}{\epsilon N^2 + \frac{\beta^2+2\epsilon c}{4}} \right\}. \tag{4.29}$$

Hence, from (4.19)–(4.21) and (4.29), we have the bound

$$|u_x - (u_N)_x| \le \left\{ \frac{c}{\pi\epsilon N} + \frac{\alpha c}{2\pi} \frac{1}{\epsilon^2 N^2 + \frac{\beta^2+2c\epsilon}{4}} + \frac{2}{1-\exp(-(\frac{\beta}{2} + \sqrt{c})\pi)} \times \frac{c}{\pi\epsilon N} + \frac{(\frac{\alpha}{\sqrt{2}} + \sqrt{c})c}{\pi} \frac{1}{\epsilon^2 N^2 + \frac{\beta^2+2c\epsilon}{4}} \right\} \exp\left(\frac{-\alpha(\pi-x) - \beta(\pi-y)}{2\epsilon}\right)$$

$$\leq \frac{3}{1-\exp(-(\frac{\beta}{2}+\sqrt{c})\pi)} \times \left\{\frac{c}{\pi\epsilon N}+\frac{(\frac{\alpha}{\sqrt{2}}+\sqrt{c})c}{\pi}\left\{\frac{1}{\epsilon^2N^2+\frac{\beta^2+2c\epsilon}{4}}\right\}\right\}\exp\left(\frac{-\alpha(\pi-x)-\beta(\pi-y)}{2\epsilon}\right).$$

The desired result (4.18) is obtained from the above estimate multiplied by ϵ. This completes the proof of Theorem 4.2. ■

For $|\varepsilon(u_y-(u_N)_y)|$ an analogous result to Theorem 4.2 is obtained by similar arguments.

With Model A for approximations to the fluxes u_x, u_y we choose N to fulfill the criterion

$$\max\left\{\max_S|\epsilon(u_x-(u_N)_x)|, \max_S|\epsilon(u_y-(u_N)_y)|\right\}\leq\delta=\frac{1}{2}10^{-4}. \tag{4.30}$$

We have the following corollary to Theorem 4.2.

Corollary 4.3. *In the case of Model A with $\alpha\geq\beta>0$, when $\epsilon\geq10^{-4}$, in order to satisfy (4.30), it suffices to choose*

$$N=O\left(\frac{1}{\sqrt{\epsilon\delta}}\right)+O\left(\frac{1}{\delta}\right). \tag{4.31}$$

Also, when $\epsilon\leq10^{-4}$ we may choose

$$N=O\left(\frac{1}{\delta}\right). \tag{4.32}$$

Corollary 4.3 implies that for Model A, it is sufficient to choose $N=O(10^4)$ in computing the approximate fluxes from (4.16) and (4.17). More interestingly, such a computation is valid for Model A even when $\epsilon\to0$.

On the other hand, in the case of Model B with $\alpha>0$ and $\beta=0$, for approximations to the fluxes u_x, u_y we choose N to fulfill the criterion

$$\max\left\{\max_S|\epsilon(u_x-(u_N)_x)|, \max_S|\sqrt{\epsilon}(u_y-(u_N)_y)|\right\}\leq\delta=\frac{1}{2}10^{-4}. \tag{4.33}$$

Note here the different scalings of the fluxes from Model A. We have the following corollary to Theorem 4.2.

Corollary 4.4. *In the case of Model B with $\beta=0$, in order to satisfy (4.33), it suffices to choose*

$$N=O\left(\frac{1}{\epsilon^{\frac{3}{4}}\sqrt{\delta}}\right)+O\left(\frac{1}{\sqrt{\epsilon}\delta}\right). \tag{4.34}$$

When $N=O(10^8)$, we may choose ϵ as small as $\epsilon=10^{-8}$ in practical computations. Compared with $N=O(10^4)$ given in Model A, more CPU time is needed. However, for the computation of scaled flux when $\epsilon\to0$, using Model A is still more beneficial, than using Model B.

5. Model C

We now consider Model C with $c=0$ and $\alpha\geq\beta>0$. In this case we have

$$T_\alpha=t_\alpha=\frac{\alpha}{2\epsilon},\qquad T_\beta=t_\beta=\frac{\beta}{2\epsilon}, \tag{5.1}$$

and (2.28)–(2.31) reduce to

$$\mathcal{L}u=-\epsilon(u_{xx}+u_{yy})+\alpha u_x+\beta u_y,\quad \text{in } S, \tag{5.2}$$

$$u(x,\pi)=u(\pi,y)=1, \tag{5.3}$$

$$u(x,0)=\frac{\sinh(\frac{\alpha}{2\epsilon}x)}{\sinh(\frac{\alpha}{2\epsilon}\pi)}\exp\left(-\frac{\alpha(\pi-x)}{2\epsilon}\right), \tag{5.4}$$

$$u(0,y)=\frac{\sinh(\frac{\beta}{2\epsilon}y)}{\sinh(\frac{\beta}{2\epsilon}\pi)}\exp\left(-\frac{\beta(\pi-y)}{2\epsilon}\right). \tag{5.5}$$

The exact solution of (5.2)–(5.5) is then given by

$$\begin{aligned}u(x,y)=\bar{u}^*(x,y)&=\frac{\sinh(\frac{\alpha}{2\epsilon}x)}{\sinh(\frac{\alpha}{2\epsilon}\pi)}\exp\left(\frac{-\alpha(\pi-x)}{2\epsilon}\right)\\&+\frac{\sinh(\frac{\beta}{2\epsilon}y)}{\sinh(\frac{\beta}{2\epsilon}\pi)}\exp\left(\frac{-\beta(\pi-y)}{2\epsilon}\right)-\frac{\sinh(\frac{\alpha}{2\epsilon}x)}{\sinh(\frac{\alpha}{2\epsilon}\pi)}\frac{\sinh(\frac{\beta}{2\epsilon}y)}{\sinh(\frac{\beta}{2\epsilon}\pi)}\exp\left(\frac{-\alpha(\pi-x)-\beta(\pi-y)}{2\epsilon}\right).\end{aligned} \tag{5.6}$$

In [5], several models with $c=0$ are discussed. The simplest model of (5.2)–(5.5) with a two-dimensional boundary layer can also be used as a test problem for comparing numerical methods. Note that there is no need for Model C to have more terms in the approximate solutions than do Models A and B, and that the conditions $\alpha>0$ and $\beta>0$ are both required for nontrivial solutions.

6. Numerical experiments with Models A, B and C

The coefficients a_k^* and b_k^* can be easily evaluated from (2.36) and (2.37). However, computations involving the exponential functions $\exp(\frac{\alpha x}{2\epsilon})$ should be avoided. In (4.1), (4.16) and (4.17), the following functions should be rewritten as

$$\frac{\sinh(t_kx)}{\sinh(t_k\pi)}=\exp(-t_k(\pi-x))\frac{(1-\exp(-2t_kx))}{(1-\exp(-2t_k\pi))}, \tag{6.1}$$

and

$$\frac{\cosh(t_kx)}{\sinh(t_k\pi)}=\exp(-t_k(\pi-x))\frac{(1+\exp(-2t_kx))}{(1-\exp(-2t_k\pi))}. \tag{6.2}$$

We choose two cases for numerical experiments: Model A with $\alpha=\beta=c=1$, whose solutions of Model A are symmetric with respect to x and y, and Model B with $\alpha=c=1$ and $\beta=0$.

First, let us verify Proposition 3.3 numerically. For Model B, the function (3.33) is simplified to

$$w(\pi,y)=f_4(y)=\frac{(\sinh\sqrt{\frac{1}{2\epsilon}}y)}{(\sinh\sqrt{\frac{1}{2\epsilon}}\pi)}-\frac{(\sinh\sqrt{\frac{1}{\epsilon}}y)}{(\sinh\sqrt{\frac{1}{\epsilon}}\pi)}. \tag{6.3}$$

By the Newton iteration method, we find the extreme location $y=\bar{y}$ and value $w(\pi,\bar{y})$. For $\epsilon=10^{-4}$, the numerical values are given by

$$\bar{y}=3.12976=\pi-\nu\sqrt{\epsilon},\qquad \nu=1.1833, \tag{6.4}$$

$$w(\pi,\bar{y})=0.12686. \tag{6.5}$$

Eqs. (6.4) and (6.5) perfectly verify Proposition 3.3. Numerical verifications of Propositions 3.1 and 3.2 can be completed similarly; the details are omitted.

Now we examine the convergence of (4.1) at $x=\pi$. Since $u(\pi,y)=1$, the required integer N can be easily determined from

$$\max_{0\le y\le\pi}|1-u_N(\pi,y)|\le\delta_d=\frac{1}{2}10^{-d},\quad d=2,3,4,5. \tag{6.6}$$

Since the extreme location $\bar{y}$ is known, we may simply seek N such that

$$|1-u_N(\pi,\bar{y})|\le\delta_d. \tag{6.7}$$

Table 6.1
The minimal N of u_N at $(x, y) = (\pi, \pi - \epsilon)$ for Model A with $\alpha = \beta = c = 1$ and $\delta_d = \frac{1}{2}10^{-d}$

ϵ	x	y	δ_2	δ_3	δ_4	δ_5
0.1	π	$\pi - \epsilon$	10	20	23	51
10^{-4}	π	$\pi - \epsilon$	0	0	0	10,588
10^{-8}	π	$\pi - \epsilon$	0	0	0	0

Table 6.2
The minimal N of u_N at $(x, y) = (\pi, \bar{y})$ for Model B with $\alpha = c = 1$, $\beta = 0$ and $\delta_d = \frac{1}{2}10^{-d}$

ϵ	x	y	δ_2	δ_3	δ_4	δ_5
0.1	π	2.76741	5	13	30	46
10^{-4}	π	3.12976	174	189	435	690
10^{-8}	π	3.14147	17,403	18,917	19,098	19,117

The computed values of N are listed in Tables 6.1 and 6.2. Based on the results in Table 6.1, the following interesting conclusions for Model A can be reached:

(1) For Model A, when $\epsilon = 10^{-8}$, $N = 0$ is given, which implies that $\bar{u}^*(x, y)$ is sufficient without more terms in the expansion. Also $N = 0$ for $\epsilon < \delta$. These results coincide with (4.14).

(2) When $\epsilon = 10^{-4}$ and $\delta = \frac{1}{2}10^{-5}$, $N = 10{,}588$ is given. In fact, $q = \frac{4}{\pi} = 1.273$, then $\epsilon > \frac{\delta}{q}$, Corollary 4.2 yields $N = \sqrt{\frac{c}{\pi\epsilon\delta}} = 25{,}231$, which is larger but not far from $N = 10{,}588$, from the viewpoint of the discrepancy between the theoretical prediction and the practical computation. In real applications in the case of Model A, we may choose $\delta = \frac{1}{2}10^{-4}$, and $N = 0$ may be used when $\epsilon = 10^{-4}$ and $\epsilon = 10^{-8}$. This is significant for practical computations of the boundary layers when $\epsilon \to 0$.

(3) When $\delta \le \frac{1}{2}10^{-4}$, $N = 23$ is listed in Table 6.1 for $\epsilon = 0.1$, which however is small. Interestingly, the convergence of Model A for $\epsilon = 0.1$ is the slowest.

From the results in Table 6.2, we can see that for Model B the smaller the value of ϵ is, the larger is the required value of N. Such a conclusion can also be drawn from (4.12). Also, the values of N given in Table 6.2 are consistent with Corollary 4.1. The maximal $N = 19{,}117$ is still small compared with that in [1].

Since the exact derivatives within S and the normal derivatives to Γ are unknown, the appropriate value of N may be found in practice from the criterion

$$|\epsilon((u_N)_x - (u_{N-1})_x)| \le \delta = \frac{1}{2}10^{-4}. \tag{6.8}$$

The resulting N and the approximate solutions and derivatives are listed in Tables 6.3–6.8. Note that $N = 1$ in (6.8) implies that $N = 0$ may be used after this trial computation. In Tables 6.3–6.8, $\epsilon(u_N)_x = O(1)$ and $\sqrt{\epsilon}(u_N)_x = O(1)$ imply that $(u_N)_x = O(\frac{1}{\epsilon})$ and $(u_N)_x = O(\frac{1}{\sqrt{\epsilon}})$ in the regular and parabolic boundary layers, respectively.

From the results in Tables 6.3–6.5, we can also see that for Model A $N = O(10)$ is needed for $\epsilon = 0.1$, but $N = 1$ suffices for $\epsilon \le 10^{-4}$. Suppose that the width of the regular layers is defined by $u_N \ge \epsilon$. A width of about 2ϵ can be observed from the solutions at $(x, y) = (\pi - i\epsilon, \pi - i\epsilon)$ in Table 6.3 for $\epsilon = 0.1$.

Suppose that the width of the parabolic boundary layers is defined by the criterion $u_N \ge \sqrt{\epsilon}$. Then a width of about $\sqrt{\epsilon}$ can be observed from the solutions at $(x, y) = (\pi - i\sqrt{\epsilon}, \pi - i\sqrt{\epsilon})$ in Table 6.6 for $\epsilon = 0.1$. For the width of the first order derivatives, the numerical width is seen to be a little larger than $2\sqrt{\epsilon}$ by noting that $\sqrt{\epsilon}(u_N)_y = 0.1360$ at $(x, y) = (\pi - 2\sqrt{\epsilon}, \pi - 2\sqrt{\epsilon})$ in Table 6.6. Thus the computational results are in close agreement with the well-known theoretical result that the width of a parabolic boundary layer is of $O(\sqrt{\epsilon})$.

It is interesting to see from Tables 6.7 and 6.8 that

$$\epsilon(u_N)_x = 0, \qquad u_N = \sqrt{\epsilon}(u_N)_y, \tag{6.9}$$

Table 6.3
The solution values near the corner (π, π) for Model A with $\alpha = \beta = c = 1$, $\delta = \frac{1}{2}10^{-4}$ and $\epsilon = 0.1$

x	y	$\epsilon(u_N)_x$	N
π	$\pi - \epsilon$	0.7454	30
π	$\pi - 2\epsilon$	0.9785	16
π	$\pi - 3\epsilon$	1.053	21
π	$\pi - 4\epsilon$	1.080	8

x	y	u_N	N	$\epsilon(u_N)_x$	N	$\epsilon(u_N)_y$	N
$\pi - \epsilon$	$\pi - \epsilon$	0.5540	18	0.2376	1	0.2376	1
$\pi - 2\epsilon$	$\pi - 2\epsilon$	0.2113	1	0.1072	1	0.1072	1
$\pi - 3\epsilon$	$\pi - 3\epsilon$	0.0738	1	3.934(−2)	1	3.934(−2)	1
$\pi - 4\epsilon$	$\pi - 4\epsilon$	0.0252	1	1.362(−2)	1	1.362(−2)	1

Table 6.4
The solution values near the corner (π, π) for Model A with $\alpha = \beta = c = 1$, $\delta = \frac{1}{2}10^{-4}$ and $\epsilon = 10^{-4}$

x	y	$\epsilon(u_N)_x$	N
π	$\pi - \epsilon$	0.6322	1
π	$\pi - 2\epsilon$	0.8648	1
π	$\pi - 3\epsilon$	0.9503	1
π	$\pi - 4\epsilon$	0.9818	1

x	y	u_N	N	$\epsilon(u_N)_x$	N	$\epsilon(u_N)_y$	N
$\pi - \epsilon$	$\pi - \epsilon$	0.6004	1	0.2326	1	0.2326	1
$\pi - 2\epsilon$	$\pi - 2\epsilon$	0.2523	1	0.1170	1	0.1170	1
$\pi - 3\epsilon$	$\pi - 3\epsilon$	0.0971	1	4.730(−2)	1	4.730(−2)	1
$\pi - 4\epsilon$	$\pi - 4\epsilon$	0.0363	1	1.797(−2)	1	1.797(−2)	1

Table 6.5
The solution values near the corner (π, π) for Model A with $\alpha = \beta = c = 1$, $\delta = \frac{1}{2}10^{-4}$ and $\epsilon = 10^{-8}$

x	y	$\epsilon(u_N)_x$	N
π	$\pi - \epsilon$	0.6321	1
π	$\pi - 2\epsilon$	0.8647	1
π	$\pi - 3\epsilon$	0.9502	1
π	$\pi - 4\epsilon$	0.9817	1

x	y	u_N	N	$\epsilon(u_N)_x$	N	$\epsilon(u_N)_y$	N
$\pi - \epsilon$	$\pi - \epsilon$	0.6004	1	0.2325	1	0.2325	1
$\pi - 2\epsilon$	$\pi - 2\epsilon$	0.2524	1	0.1170	1	0.1170	1
$\pi - 3\epsilon$	$\pi - 3\epsilon$	0.0971	1	4.731(−2)	1	4.731(−2)	1
$\pi - 4\epsilon$	$\pi - 4\epsilon$	0.0363	1	1.798(−2)	1	1.798(−2)	1

at $(x, y) = (\bar{x}, \bar{y}) = (\pi - i\sqrt{\epsilon}, \pi - i\sqrt{\epsilon})$, $i = 1, 2, 3, 4$. Eq. (6.9) implies that for $x \in [\pi - \sqrt{\epsilon}, \pi - 4\sqrt{\epsilon}]$, the solution $\hat{u}(y) = u_N$ is independent of x, and satisfies

$$\hat{u} = \sqrt{\epsilon}\frac{\mathrm{d}\hat{u}}{\mathrm{d}y}, \qquad \hat{u}|_{y=\pi} = 1. \tag{6.10}$$

The solution of the above equation is given by

$$\hat{u} = \exp\left(-\frac{1}{\sqrt{\epsilon}}(\pi - y)\right). \tag{6.11}$$

Table 6.6
The solution values near the corner (π, π) in the distance of $O(\sqrt{\epsilon})$ for Model B with $\alpha = c = 1$, $\beta = 0$, $\delta = \frac{1}{2}10^{-4}$ and $\epsilon = 0.1$

x	y	$\epsilon(u_N)_x$	N	x	y	$\sqrt{\epsilon}(u_N)_y$	N
π	$\pi - \sqrt{\epsilon}$	0.7179	20	$\pi - \sqrt{\epsilon}$	π	0.9787	20
π	$\pi - 2\sqrt{\epsilon}$	0.9564	35	$\pi - 2\sqrt{\epsilon}$	π	1.000	5
π	$\pi - 3\sqrt{\epsilon}$	1.041	33	$\pi - 3\sqrt{\epsilon}$	π	1.000	1
π	$\pi - 4\sqrt{\epsilon}$	1.073	47	$\pi - 4\sqrt{\epsilon}$	π	1.000	1
x	y	u_N	N	$\epsilon(u_N)_x$	N	$\sqrt{\epsilon}(u_N)_y$	N
$\pi - \sqrt{\epsilon}$	$\pi - \sqrt{\epsilon}$	0.3852	8	1.960(−2)	9	0.3549	10
$\pi - 2\sqrt{\epsilon}$	$\pi - 2\sqrt{\epsilon}$	0.1360	1	7.887(−4)	1	0.1351	1
$\pi - 3\sqrt{\epsilon}$	$\pi - 3\sqrt{\epsilon}$	4.981(−2)	1	2.996(−5)	1	4.978(−2)	1
$\pi - 4\sqrt{\epsilon}$	$\pi - 4\sqrt{\epsilon}$	1.832(−2)	1	1.038(−6)	1	1.832(−2)	1

Table 6.7
The solution values near the corner (π, π) in the distance of $O(\sqrt{\epsilon})$ for Model B with $\alpha = c = 1$, $\beta = 0$, $\delta = \frac{1}{2}10^{-4}$ and $\epsilon = 10^{-4}$

x	y	$\epsilon(u_N)_x$	N	x	y	$\sqrt{\epsilon}(u_N)_y$	N
π	$\pi - \sqrt{\epsilon}$	0.5070	1	$\pi - \sqrt{\epsilon}$	π	1.000	1
π	$\pi - 2\sqrt{\epsilon}$	0.7570	1	$\pi - 2\sqrt{\epsilon}$	π	1.000	1
π	$\pi - 3\sqrt{\epsilon}$	0.8802	1	$\pi - 3\sqrt{\epsilon}$	π	1.000	1
π	$\pi - 4\sqrt{\epsilon}$	0.9410	1	$\pi - 4\sqrt{\epsilon}$	π	1.000	1
x	y	u_N	N	$\epsilon(u_N)_x$	N	$\sqrt{\epsilon}(u_N)_y$	N
$\pi - \sqrt{\epsilon}$	$\pi - \sqrt{\epsilon}$	0.3679	1	1.858(−44)	1	0.3679	1
$\pi - 2\sqrt{\epsilon}$	$\pi - 2\sqrt{\epsilon}$	0.1353	1	1.024(−87)	1	0.1353	1
$\pi - 3\sqrt{\epsilon}$	$\pi - 3\sqrt{\epsilon}$	4.979(−2)	1	4.389(−131)	1	4.979(−2)	1
$\pi - 4\sqrt{\epsilon}$	$\pi - 4\sqrt{\epsilon}$	1.832(−2)	1	1.729(−174)	1	1.832(−2)	1

Table 6.8
The solution values near the corner (π, π) in the distance of $O(\sqrt{\epsilon})$ for Model B with $\alpha = c = 1$, $\beta = 0$, $\delta = \frac{1}{2}10^{-4}$ and $\epsilon = 10^{-8}$

x	y	$\epsilon(u_N)_x$	N	x	y	$\sqrt{\epsilon}(u_N)_y$	N
π	$\pi - \sqrt{\epsilon}$	0.5069	1	$\pi - \sqrt{\epsilon}$	π	1.000	1
π	$\pi - 2\sqrt{\epsilon}$	0.7569	1	$\pi - 2\sqrt{\epsilon}$	π	1.000	1
π	$\pi - 3\sqrt{\epsilon}$	0.8801	1	$\pi - 3\sqrt{\epsilon}$	π	1.000	1
π	$\pi - 4\sqrt{\epsilon}$	0.9409	1	$\pi - 4\sqrt{\epsilon}$	π	1.000	1
x	y	u_N	N	$\epsilon(u_N)_x$	N	$\sqrt{\epsilon}(u_N)_y$	N
$\pi - \sqrt{\epsilon}$	$\pi - \sqrt{\epsilon}$	0.3679	1	0.0000	1	0.3679	1
$\pi - 2\sqrt{\epsilon}$	$\pi - 2\sqrt{\epsilon}$	0.1353	1	0.0000	1	0.1353	1
$\pi - 3\sqrt{\epsilon}$	$\pi - 3\sqrt{\epsilon}$	4.979(−2)	1	0.0000	1	4.979(−2)	1
$\pi - 4\sqrt{\epsilon}$	$\pi - 4\sqrt{\epsilon}$	1.832(−2)	1	0.0000	1	1.832(−2)	1

On the other hand, for Model B with $\alpha = c = 1$ and $\beta = 0$, when $\epsilon \to 0$ the solution (2.26) at $(\bar{x}, \bar{y})$ leads to

$$u^*(\bar{x}, \bar{y}) \approx \frac{\sinh(\frac{1}{\sqrt{\epsilon}}y)}{\sinh(\frac{1}{\sqrt{\epsilon}}\pi)} \approx \exp\left(-\frac{1}{\sqrt{\epsilon}}(\pi - y)\right). \tag{6.12}$$

The observed results (6.9) are reasonable because $\hat{u} \approx \bar{u}^*$. We can also conclude from (6.9) that, when $x \le \pi - \sqrt{\epsilon}$, the two-dimensional problem Model B may be simplified to the one-dimensional problem

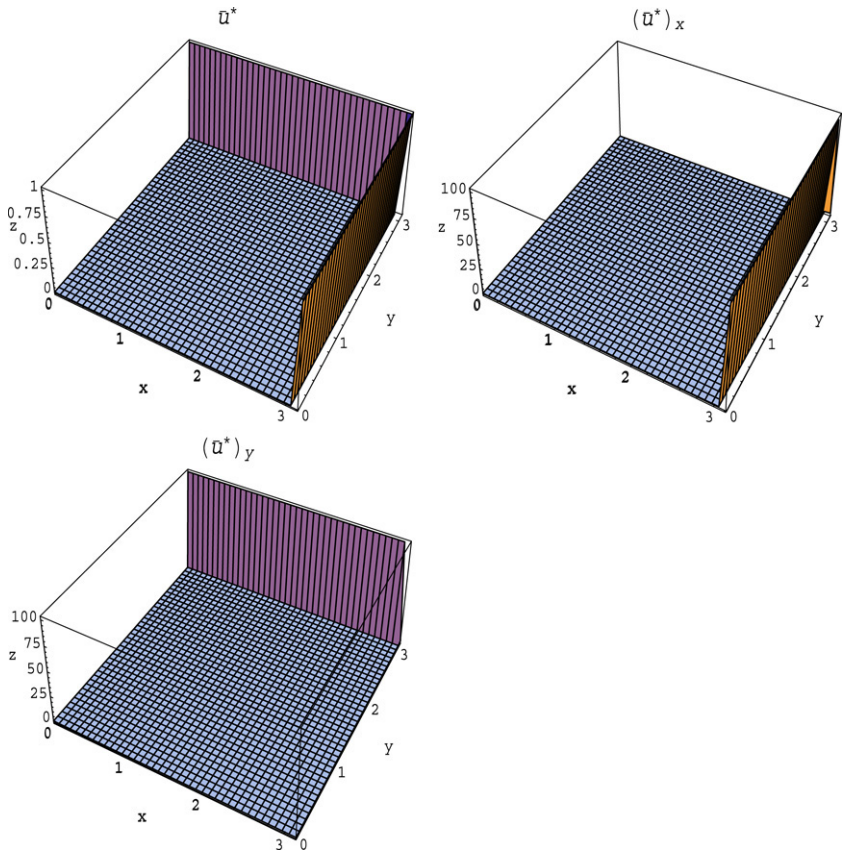

Fig. 6.1. The profiles of the solutions and derivatives for Model A with $\alpha = \beta = c = 1$ and $\epsilon = 0.01$.

$$-\epsilon w''(y) + cw(y) = 0, \qquad w(0) \approx 0, \qquad w(\pi) = 1 \tag{6.13}$$

with the solution $w(y) = \exp(-\frac{1}{\sqrt{\epsilon}}(\pi - y))$. The solution behaviour of Model B is more complicated and intriguing than that of Model A; more detailed numerical results are reported in [1].

The solution profiles of $\bar{u}^*$ (i.e., $N = 0$) for Models A, B and C are depicted in Figs. 6.1–6.3, where $u = \bar{u}^*$ for Model C. We depict the solution profiles for only $\epsilon = 0.01$. It is easy to see that the widths of the parabolic boundary layers in Fig. 6.2 are much larger than those of the regular boundary layers in Fig. 6.1. It can also be observed from the results in Fig. 6.2 that for Model B there exists a discrepancy between $\bar{u}^*$ and $u = 1$ along $x = \pi$, which is consistent with Proposition 3.3, where $\min \bar{u}^* = 1 - 0.1268 = 0.8732$ at $x = \pi$. Figs. 6.1–6.3 show that Models A, B and C are good examples of singularly perturbed problems that have solutions containing two-dimensional boundary layers, and thus that they can serve as better test problems than Model I in [1].

7. Final remarks

(a) In this paper accurate and approximate analytic solutions of three new test problems, called Models A, B and C, for singularly perturbed differential equations were considered. The approximate analytic solutions of Models A and B have much faster convergence rates than those for Model I in [1]. For Model B the termination integer for the relative errors of u_N, and its fluxes, is $N = O(\frac{1}{\epsilon^{\frac{3}{4}}\sqrt{\delta}})$. Hence we may choose $\epsilon = 10^{-8}$ in real computations. Note that the fast convergence of u_N, $\epsilon(u_N)_x$ and $\epsilon(u_N)_y$ in this paper is valid over the entire domain S including the corner (π, π). This is significant, compared with Model I in [1,8], where the flux computation at the corner (π, π) is excluded.

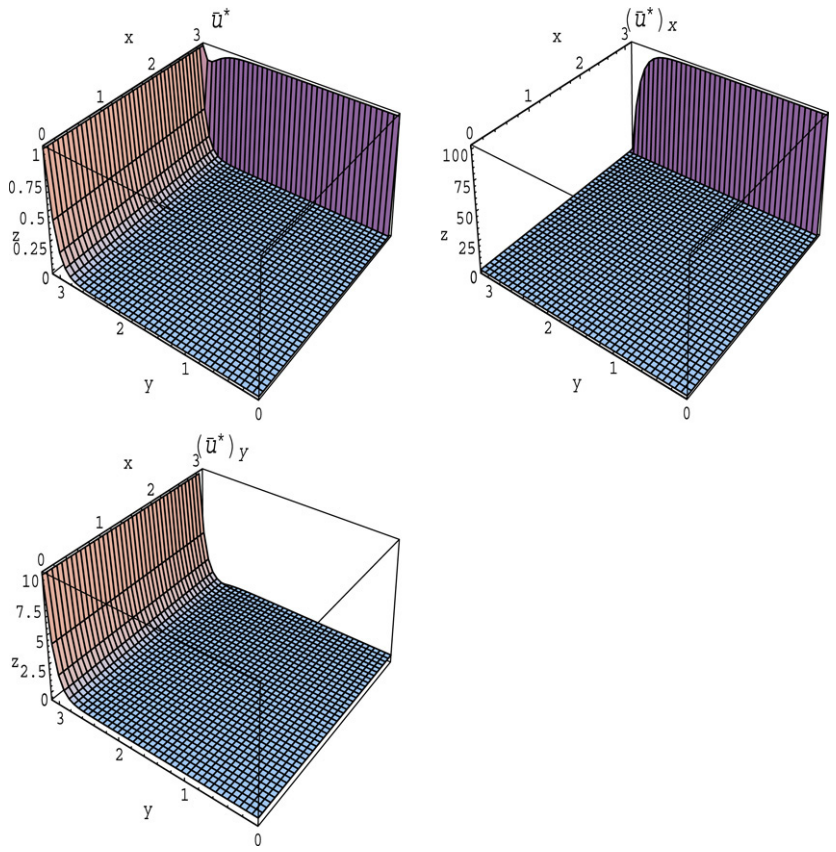

Fig. 6.2. The profiles of the solutions and derivatives for Model B with $\alpha = c = 1$, $\beta = 0$ and $\epsilon = 0.01$.

(b) Interestingly, for Model A we may carry out the computation of u_N, $\epsilon(u_N)_x$ and $\epsilon(u_N)_y$ even for $\epsilon \to 0$, see Corollaries 4.2 and 4.3. Moreover, when $N = O(10^4)$, the approximate solutions are satisfactory for practical applications.

(c) The computed results in Section 6 are promising. For $\delta = \frac{1}{2}10^{-4}$, we may choose $N = 0$ for Model A when $\epsilon \leq 10^{-4}$. This implies that the function $\bar{u}^*(x, y)$ in (2.26) can be chosen as the approximate solution of Model A, and there is no need for further terms in the expansion. This is particularly significant for regular boundary layers as $\epsilon \to 0$. The maximal N are found numerically to be

$$N = O(10), \qquad N = O(10^4), \tag{7.1}$$

for Models A, B respectively. Fast convergence rates of the test problems are essential in applications. Hence, Models A and B and the corresponding analysis in this paper will provide an impact on the study of numerical methods for singularly perturbed differential equations. All computations in Tables 6.1–6.8 are carried out by Java programs in double precision, in contrast to those in [1] carried out by Mathematica programs, using an unlimited number of significant digits.

(d) In [1] the fundamental analysis of approximate analytic solutions of some singularly perturbed differential equations was reported. Model I with two-dimensional boundary layers and Model II with spike-like solutions were proposed. In the present paper, we constructed additional approximate analytic solutions in Section 2.1, and we deliberately designed Models A and B with two-dimensional boundary layers such that their approximate solutions have fast convergence rates. Model C has a simple exact solution in the case $c = 0$. Other better and more useful test problems for singularly perturbed differential equations may be found in the future by following the techniques described in this paper and in [1].

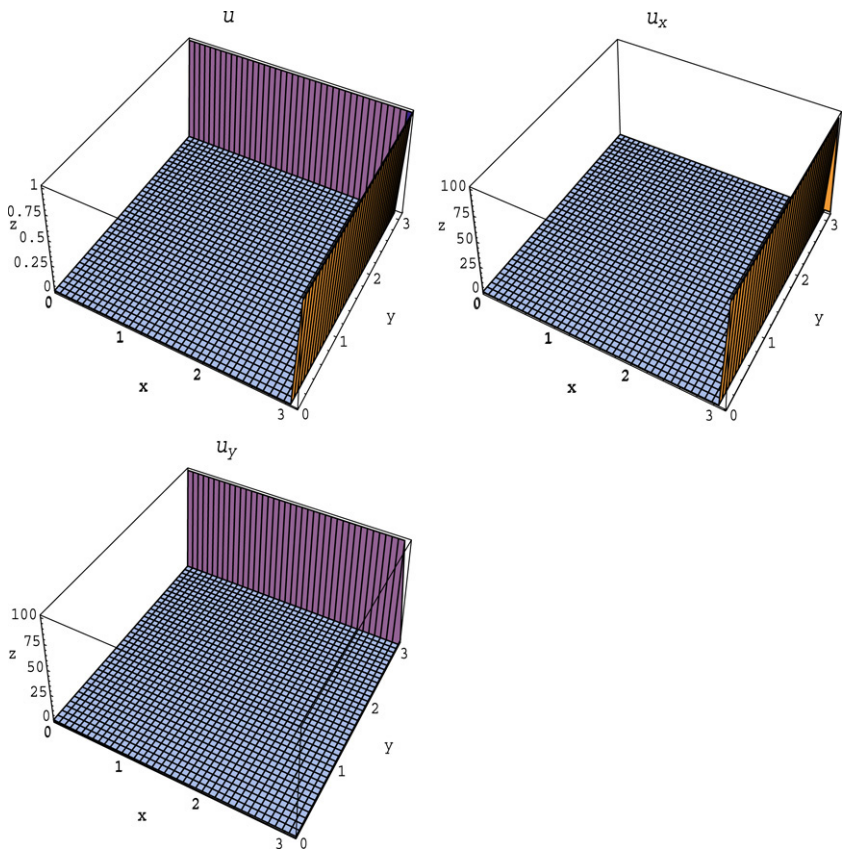

Fig. 6.3. The profiles of the solutions and derivatives for Model C with $\alpha = \beta = 1$, $c = 0$ and $\epsilon = 0.01$.

Acknowledgments

We are grateful to Prof. T.T. Lu and Dr. H.Y. Hu for their valuable suggestions and help for the work related to this paper.

References

[1] Z.C. Li, H.Y. Hu, C.H. Hsu, S. Wang, Particular solutions of singularly perturbed partial differential equations with constant coefficients in rectangular domains, I. Convergence analysis, J. Comput. Appl. Math. 166 (2004) 181–208.
[2] J.J.H. Miller, S. Wang, A new non-conforming Petrov-Galerkin finite element method with triangular elements for a singularly perturbed advection-diffusion problem, IMA J. Numer. Anal. 14 (1994) 257–276.
[3] H.G. Roos, M. Stynes, L. Tobiska, Numerical Methods for Singularly Perturbed Differential Equations, in: Convection-Diffusion and Flow Problems, Springer, 1996.
[4] J.J.H. Miller, E. O'Riordan, G.I. Shishkin, Fitted Numerical Methods for Singular Perturbation Problems, World Scientific, Singapore, 1996.
[5] P.A. Farrell, A.F. Hegarty, J.J.H. Miller, E. O'Riordan, G.I. Shishkin, Robust Computational Techniques for Boundary Layers, Chapman & Hall/CRC, Boca Raton, London, 2000.
[6] S. Wang, Z.C. Li, An analysis of a conforming exponentially fitted triangular finite element method for a singularly perturbed convection-diffusion equation, J. Comput. Appl. Math. 143 (2002) 291–310.
[7] S. Wang, Z.C. Li, A non-conforming combination of the finite element and volume methods for a singularly perturbed convection-diffusion equation, Math. Comp. 72 (2003) 1689–1709.
[8] H.Y. Hu, H.S. Tsai, Z.C. Li, S. Wang, Particular solutions of singularly perturbed partial differential equations with constant coefficients in rectangular domains, II. Computational aspects, Technical Report, Department of Applied Mathematics, National Sun Yat-sen University, 2004.
[9] G. Grunberg, A new method of solution of certain boundary problems for equations of mathematical physics permitting of separation of variables, J. Phys. 10 (1946) 301–320.
[10] S. Gradshteyn, I.M. Ryzhik, Table of Integrals, Series, and Products, Corrected and Enlarged Edition, Academic Press, New York, 1980.